In this study we are interested by the station design in term of parameter accuracy, and more particularly on the accuracy of the azimuth. In short, in presence of only pure coherent acoustic waves, it is clear that the best design is to locate sensors at far as possible. For which reason could we take into account an upper bound on the aperture ?

Regarding the size of the station and the distance of the source, a possible phenomena, which could induce a limitation on the station aperture in presence of a coherent acoustic signal, is that the loss of coherence (LOC) which usually increases when the distance between sensors increases.

For conducting this study the 3 points following program has been considered:

- choosing an index to evaluate the accuracy of the station. A commonly used index is the Cramer-Rao bound (CRB). Typically that depends on the geometry of the station, the level of noise and the LOC features. A summary of the CRB could be the area/volume of the confidence ellipsoid.

- choosing features to characterize a geometry. We have retained (i) the isotropy and (ii) the uniform distribution of the inter-distances. The isotropy is easy to check and also it is simple to correct if necessary by adding 2 sensors (resp. 3) for 2D station (resp. 3D station).

  We can not answer to the good effect or not of the inter-distance uniformity because that depends on the LOC model. Therefore we have to validate a such model.

- validating a LOC model.

  The used LOC feature is the magnitude square coherence (MSC). This index has the interesting property to be between 0 and 1, and equal to 1 iff the two signals are spatially coherent.

  The approach to determine the LOC model is based on the observation analysis. It is conducted as it follows: we consider the station I37 which consists of 10 sensors with 45 uniformly disibuted inter-distances. We base the analysis on the presence of a quasi-permanent coherent acoustical signal, saying the microbarom, in a frequency bandwidth large enough between 0.05 to 3 Hz.

  For a given frequency, we select the portions of signals where the MSC is greater than 0.8 on the three nearest sensors and study the decay of the MSC along the inter-distance values.

Remark 1 (on the noise) *Typical station aperture is 2 km. Noise is mainly due to the wind.*

- *Therefore we assume that the noises are spatially uncorrelated regarding the sensor inter-distances.*

- *On the other hand, we assume that the noise levels are identical on all sensors. Although that is not realistic, it is worth to notice that the noise level is not directly related to the inter-distances between sensors. It follows that, for the station design understanding, we can consider there is no loss of generalities to assume that.*

Remark 2 (on the coherent source) *To be able to study the LOC, we need a permanent source. The microbarom plays this role in the following.*

Remark 3 (on the isotropy) *In the absence of LOC, the station is isotrope iff*

$$XX^T \propto I_d \tag{1}$$

where X is $d \times M$ matrix whose the m-th colomun if the coordinates of the m-th sensor (in any system of coordinates).

It follows that given an arbitrary array with M sensors in $\mathbb{R}^d$ it is always possible to complete with d locations in such a way the new array is isotrope, i.e. verifies (1)*, see annex.*

Remark 4 (on the geometry) *In the absence of LOC, we will see below that the best performances are associated with inter-distances as large as possible. In this case the maximization of the minimal distance leads to locate the sensors on a circle. But in this case the distribution of the distances is not uniform. It follows that in presence of LOC, several sensors are concern with the same LOC. It seems (it is not a proof) that a rule could be to locate the sensors in such a way that the distances are more uniform (see figure 1).*

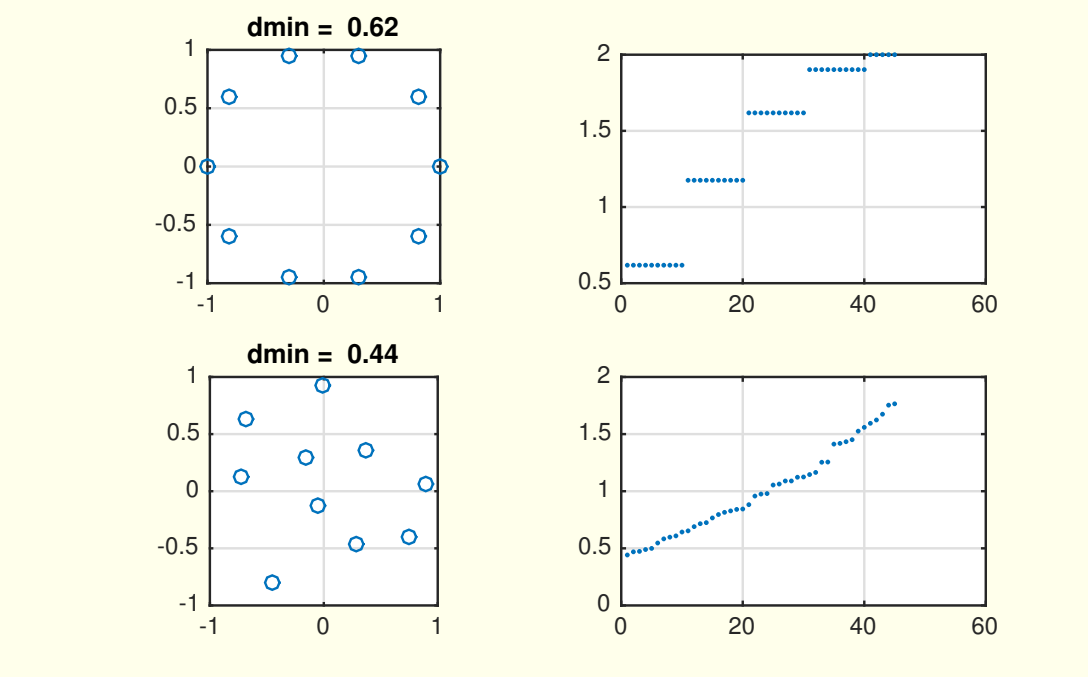

Figure 1: *Sensor locations with inter distances*

1 LOC model

1.1 Case of 2 sensors

By definition, two signals arriving on a two different locations are said non-coherent signals, or called noises, if they are spatially uncorrelated. More specifically if $x_1(t)$ and $x_2(t)$ denote the respective stationary signals observed in to different locations, the coherence level is defined by the magnitude square coherence:

$$\mathrm{MSC}(f) \quad = \quad \frac{|S_{12}(f)|^2}{S_{11}(f)S_{22}(f)}$$

where $S_{11}(f)$ and $S_{22}(f)$ denote the spectral densities of $x_1(t)$ and $x_2(t)$, and $S_{12}(f)$ the cross-spectrum. It is well known that $\mathrm{MSC}(f) \leq 1$.

Definition 1 (coherence - I) *When* $\mathrm{MSC}(f) = 1$, *we say that the 2 signals are perfectly coherent, elsewhere we speak about loss of coherence (LOC).*

It is shown that the $\mathrm{MSC}(f)$ between the two signals is 1, if and only if it exists a filter, whose impulse respond is denoted $g(t)$, such that $x_1(t) = g_1(t) \star x_2(t)$. A particular case is $g(t) = \delta(t - t_0)$ which corresponds to the pure delay t_0.

When $\mathrm{MSC}(f) = 0$ we say that the 2 signals are spatially uncorrelated and are called noises.

1.2 Case of M sensors

We consider a station with M sensors. There is only one acoustic source faraway from the station, in such a way it can be considered as planar wave. This source is called in the following signal of interest (SOI). Therefore the M-ary signal writes:

$$x(t) \quad = \quad \underbrace{s(t;\theta)}_{\text{SOI: acoustic signal}} + \underbrace{w(t)}_{\text{noise}}$$

where θ denotes the 3D slowness vector. Under pure delay assumption we can write for the m-th sensor located in r_m:

$$s_m(t;\theta) \quad = \quad s(t - r_m^T\theta) \tag{2}$$

It follows that, under the assumption that $s(t)$ is stationary random process with spectral density $\gamma_s(f)$, the spectral matrix of the M-ary process $s(t)$, whose the m-th entry is (2), writes:

$$\Gamma_s(f) \quad = \quad \gamma_s(f)d(f)d^H(f)$$

where $d(f)$ is a M-ary vector whose the m-entry writes $e^{-2j\pi f r_m^T\theta}$. Clearly the matrix $\Gamma_s(f)$ is of rank 1. That represents the general definition of the coherence.

Definition 2 (coherence - II) *M stationary signals are said coherent if their spectral matrix is of rank 1 .*

This definition is in accordance with the definition 1 given for 2 sensors.

Theorem 1 (fundamental property) *For any frequency f, the spectral matrix is positive.*

We assume that the M-ary noise $w(t)$ is temporally and spatial white. That writes $\mathbb{E}\left[w(t)w^T(t')\right] = \sigma^2\delta(t-t')$, therefore its spectral matrix writes $\sigma^2 I_M$ for any frequency. Assuming that the noise and the SOI are not correlated, it follows that the spectral matrix of the observation writes $\Gamma_x(f) = \gamma_s(f)d(f)d^H(f) + \sigma^2 I_M$ that can be rewritten:

$$\Gamma_x(f) \;=\; \gamma_s(f)D(f)C(f)D^H(f) + \sigma^2 I_M \tag{3}$$

where $D(f)$ is an M-ary diagonal matrix whose the m-th diagonal entry writes $D_{m,m} = e^{-2j\pi f r_m^T \theta}$ and where $C(f) = \mathbb{1}\mathbb{1}^T$. The LOC is then characterized by a matrix $C(f)$ which is no more of rank 1, but must be positive and with diagonal element equal to 1. This expression can be a little bit more generalized:

$$\Gamma_x(f) \;=\; D(f)\Gamma_s(f)C(f)\Gamma_s(f)D^H(f) + \sigma^2 I_M$$

where $\Gamma_s(f)$ is a diagonal matrix whose the m-th diagonal entry is $\gamma_{s,m}^{1/2}(f)$ meaning that the SOI arrives on each sensor with different spectral content. That is not considered in the following. We only consider that $\gamma_{s,m}(f) = \gamma_s(f)$ does not depend on m.

It follows that, for a pure delay and in the absence of LOC, taken $C(f) = \mathbb{1}\mathbb{1}^T$ in expressed in (3), the MSC between any sensor pair (m, m') writes:

$$\mathrm{MSC}_{m,m'}(f) \;=\; \frac{\gamma_s^2(f)}{(\gamma_s(f)+\sigma^2)(\gamma_s(f)+\sigma^2)}$$

Therefore, in presence of noise, the MSC level is no more equal to 1. In more general case:

$$\mathrm{MSC}_{m,m'}(f) \;=\; \frac{\gamma_s^2(f)\, C_{m,m'}(f)}{(\gamma_s(f)+\sigma^2)(\gamma_s(f)+\sigma^2)}$$

Remark 5 *Coherence is not only restricted to the case of pure delays. Perfect coherence is also verified for filtering signals.*

Remark 6 *Noise induces a LOC.*

1.3 Discrete domain

All signals are real and sampled at the sampling frequency $F_s = 20$ Hz. After sampling we obtain $x_n = x(n/F_s)$. For $k = 0$ to $(N-1)$ we consider the M-ary discrete Fourier transform:

$$X_k \;=\; \frac{1}{\sqrt{N}} \sum_{n=0}^{N-1} x_n\, e^{-2j\pi n f_k} \quad \text{where} \quad f_k = kF_s/N$$

We let $K = N/2$. For K great enough, X_1, ..., X_K is a sequence of M-ary independent circularly gaussian random vectors with zero-mean and respective covariance:

$$\Gamma_k(\alpha) \;=\; \gamma_k d_k(\theta) d_k^H(\theta) + \sigma^2 I_M \tag{4}$$

where $d_k(\theta)$ is an M-ary vector whose the m-th entry writes $D_{k,m} = e^{-2j\pi f_k r_m^T \theta}$ and where $\gamma_k = \gamma_s(f_k)$.

The expression (4) can be rewritten:

$$\Gamma_k(\alpha) \;=\; \gamma_k D_k(\theta)\, C_k\, D_k^H(\theta) + \sigma^2 I_M \tag{5}$$

where $D_k(\theta)$ is an M-ary diagonal matrix whose the m-th diagonal entry writes $D_{k,m,m'} = e^{-2j\pi f_k r_m^T \theta}$ and where $C_k = \mathbb{1}\mathbb{1}^T$ which is a rank 1 matrix. Under LOC, C_k is no more a rank 1 projector, but must be positive and such that $C_{k,m,m} = 1$.

From (5), we get:

$$\Gamma_{k,m,m'} \;=\; \gamma_k C_{k,m,m'} e^{-2j\pi f_k (r_m - r_{m'})^T \theta} + \sigma^2 \delta_{m,m'}$$

We let $\mathrm{SNR}_k = \gamma_k/\sigma^2$ the signal-to-noise ratio at the frequency f_k. It follows that the MSC at the frequency f_k between any two sensors writes:

$$\mathrm{MSC}_{k,m,m'} \;=\; \frac{1}{(1+\mathrm{SNR}_k^{-1})^2}\, |C_{k,m,m'}|^2 \tag{6}$$

It follows that the MSC could be less than 1 on one hand to the presence of noise and on the other to the LOC of the acoustic wave.

A commonly used model for the LOC of the acoustic source is for $1 \leq m \leq M$ and $1 \leq m' \leq M$:

$$C_{k,m,m'} \;=\; e^{-2\pi^2 f_k^2 (r_m - r_{m'})^T S_\theta (r_m - r_{m'})} \tag{7}$$

where S_θ is a 3×3 covariance matrix depending on 3 free parameters. Using (6), we get:

$$\log \mathrm{MSC}_{k,m,m'} \;=\; -2\log(1+\mathrm{SNR}_k^{-1}) - 4\pi^2 f_k^2 (r_m - r_{m'})^T S_\theta (r_m - r_{m'})$$

In the simple case where S_θ is proportional to the identity, this expression simplifies as:

$$\log \mathrm{MSC}_{k,m,m'} \;=\; \beta_0 + \beta_1 f_k^2 d_{m,m'}^2 \tag{8}$$

where we have assumed that the SNR does not depend on k and writes:

$$\mathrm{SNR} \;=\; \frac{1}{e^{-\beta_0/2} - 1}$$

Likelihood function

In summary we can write that:

$$(X_1, \ldots, X_K) \;\sim\; \prod_{k=1}^{K} \mathcal{N}_c(x_k; 0_M, \Gamma_k(\alpha))$$

and the likelihood writes:

$$\mathcal{L}(\alpha) \;=\; \sum_{k=1}^{K} \log\det \Gamma_k(\alpha) + \mathrm{trace}\left(\Gamma_k^{-1}(\alpha) X_k X_k^T\right) \tag{9}$$

where the parameter α consists of

$$\alpha \;=\; \{\theta_1, \theta_2, \theta_3, \gamma_1, \ldots, \gamma_K, S_\theta, \sigma^2\} \in \mathbb{R}^3 \times \mathbb{R}^{+K} \times \mathcal{M}_3^+ \times \mathbb{R}^+ \tag{10}$$

where $\mathcal{M}_3^+$ is the set of 3×3 positive matrices. The size of the parameter α is $K + 7$ whereas the number of observations is $2MK$.

Another way is to characterize the slowness by azimuth, elevation and velocity and the LOC by the respective standard deviations of them, see expression (B.1).

2 LOC study: numerical results

The objective of this section is to validate, by numerical results, the simple relationship between the LOC and the distance given by the expression (8), that we rewrite below:

$$\log \mathrm{MSC}_{k,m,m'} \quad = \quad \beta_0 + \beta_1 f_k^2 d_{m,m'}^2$$

It is worth to notice that β_0 is related to the SNR level at the frequency k. Here for sake of simplicity we assume that this SNR does not depend on the frequency. That could be well verified if the bandwidth of the SOI is narrow enough.

To studying this LOC model we need (i) a station with a large number of sensors located in such a way that the distribution of the inter-distances is quiet uniform, (ii) a coherent source almost permanently present. A good example is the microbarom, but unfortunately it covers a small part of the frequency bandwidth of interest.

Figure 2, we observe an almost permanent component around 0.04 Hz and another around 0.28 Hz. We also observe bursts in red in the low frequency. These bursts present a low coherence between them as we see figure 12.

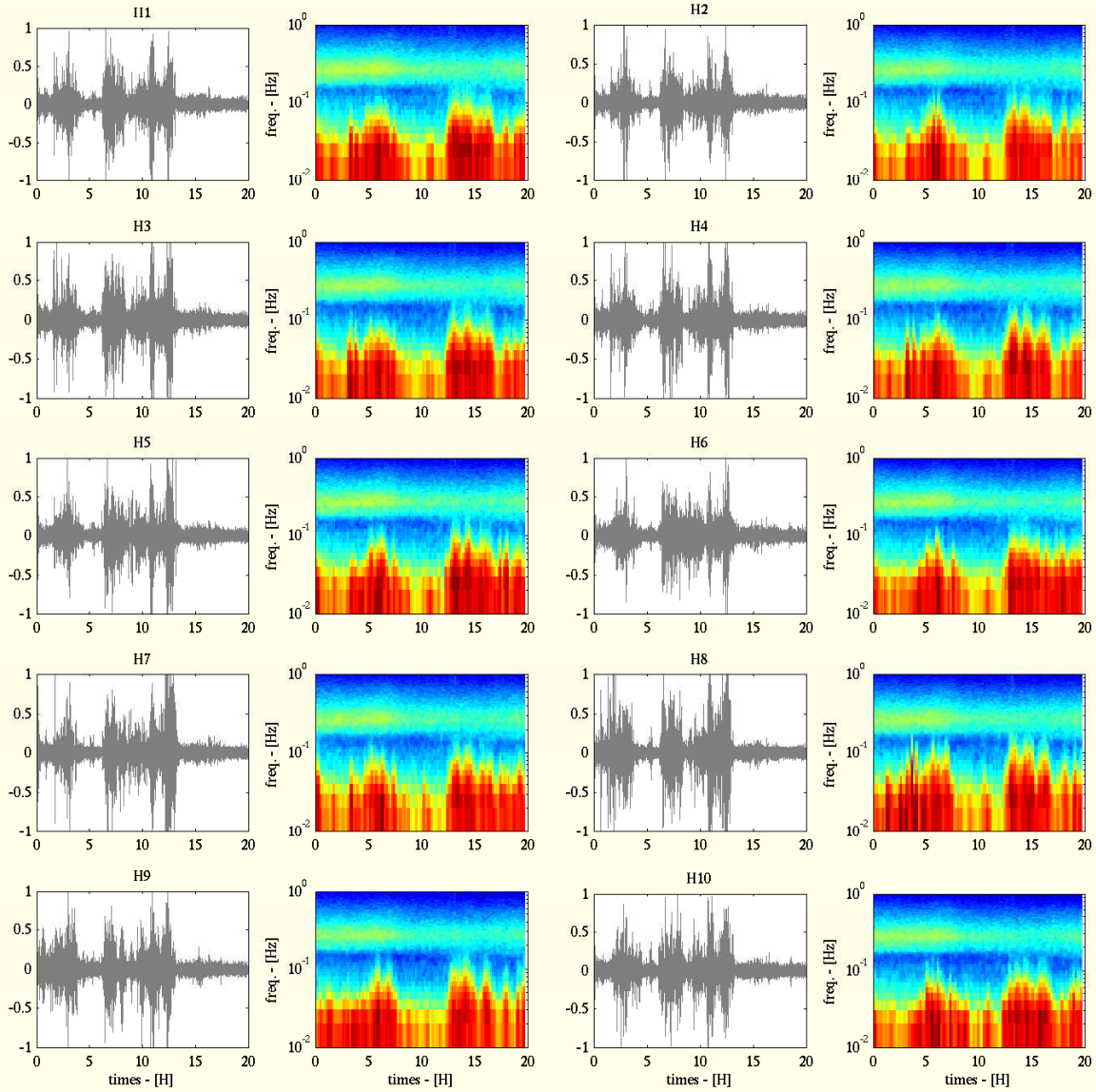

Figure 2: *Typical observations on I37 during about* 20 *hours. The signals are filtered in the band* 0.01 *Hz to* 4 *Hz. The plot im grey represents the time observations. The color image represents the spectral analysis. The time wimdows is* 500 *seconds. We observe an almost permanent component below* 0.1 *Hz and another around* 0.28 *Hz.*

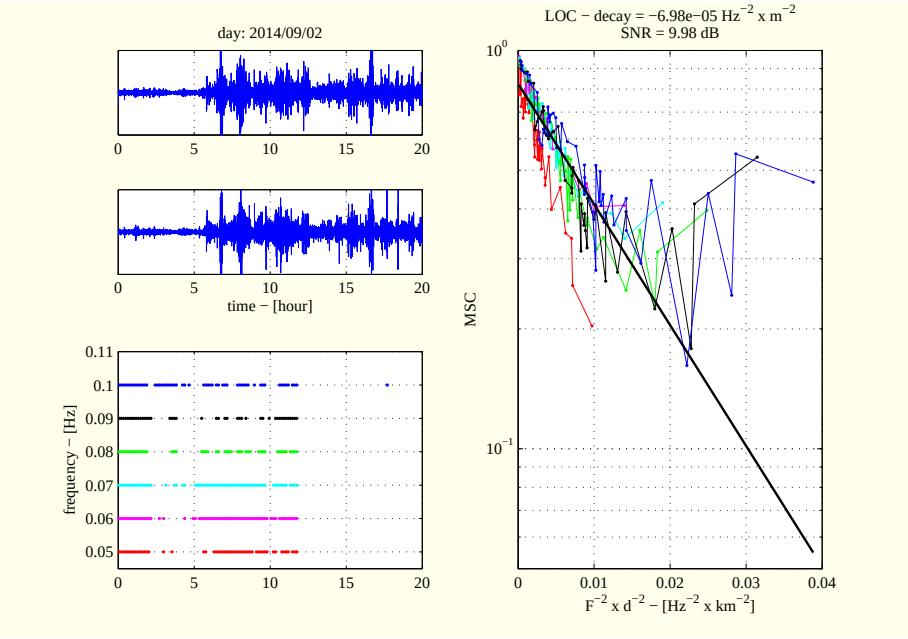

Figure 3: *LHS figures: on top, the two nearest sensor signals. Bottom: time slots where the MSC is greater than* 0.9 *for different frequencies in the band* 0.05 *Hz to* 0.1 *Hz. RHS figure: the decay of the MSC for the different frequencies reported on the LHS bottom figure as a function of the* $10 \times 9/2 = 45$ *values of* $f^2 d^2$*. In the model given by* (8)*, the intercept is related to the SNR.*

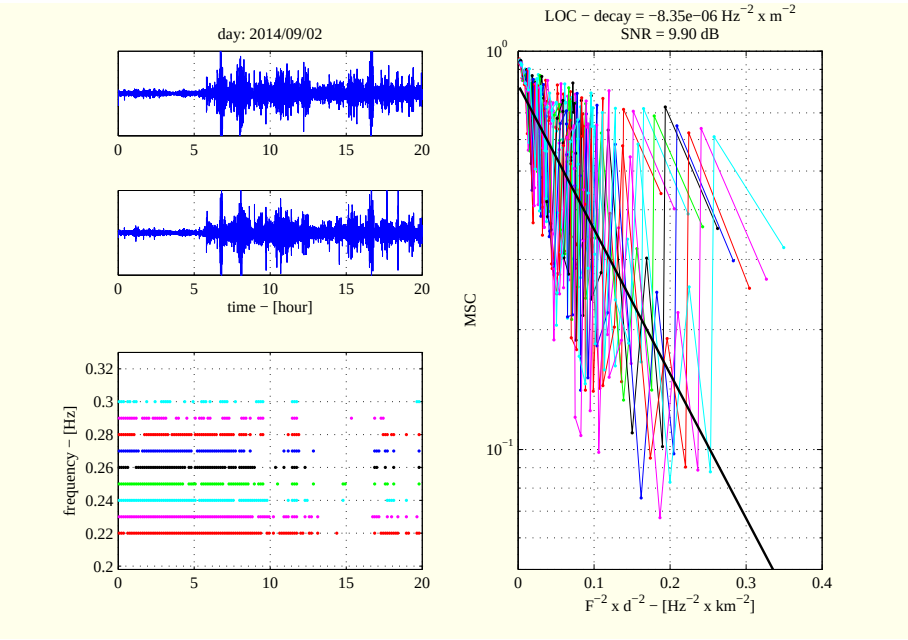

Figure 4: *LHS figures: on top, the two nearest sensor signals. Bottom: time slots where the MSC is greater than* 0.9 *for different frequencies in the band* 0.25 *Hz to* 0.3 *Hz. RHS figure: the decay of the MSC for the different frequencies reported on the LHS bottom figure as a function of the* $10 \times 9/2 = 45$ *values of* $f^2 d^2$*. In the model given by* (8)*, the intercept is related to the SNR.*

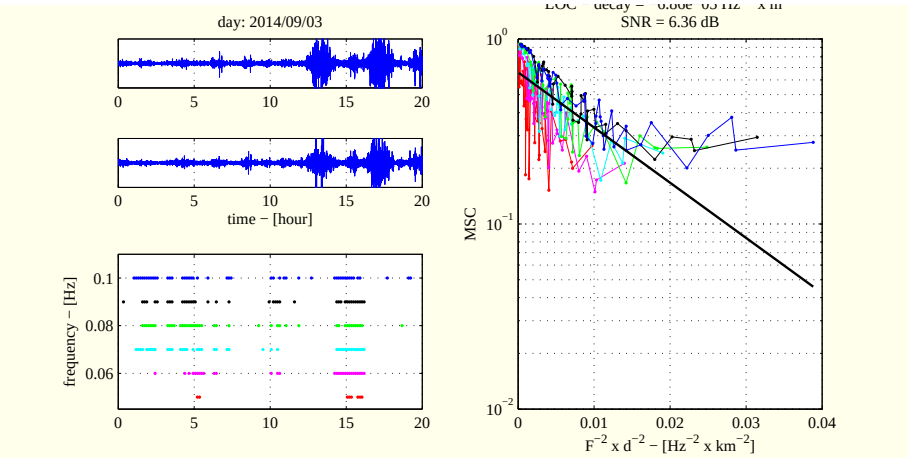

Figure 5: *LHS figures: on top, the two nearest sensor signals. Bottom: time slots where the MSC is greater than* 0.9 *for different frequencies in the band* 0.05 *Hz to* 0.1 *Hz. RHS figure: the decay of the MSC for the different frequencies reported on the LHS bottom figure as a function of the* $10 \times 9/2 = 45$ *values of* $f^2 d^2$*. In the model given by* (8)*, the intercept is related to the SNR.*

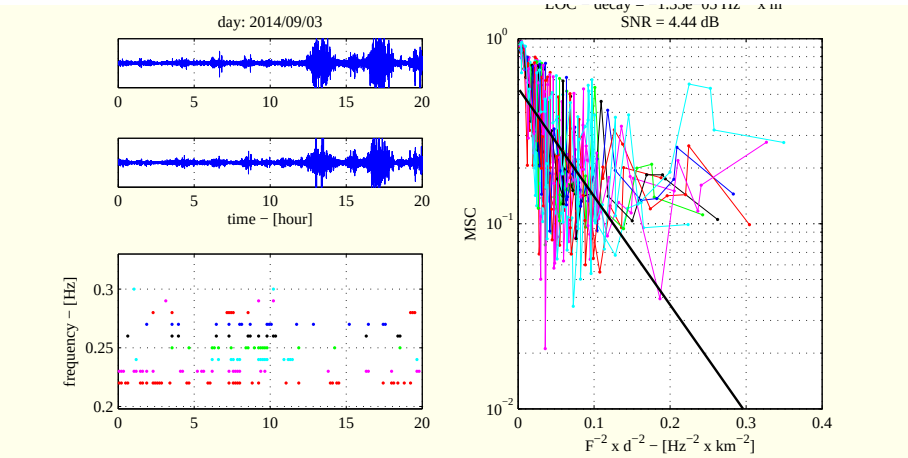

Figure 6: *LHS figures: on top, the two nearest sensor signals. Bottom: time slots where the MSC is greater than* 0.9 *for different frequencies in the band* 0.25 *Hz to* 0.3 *Hz. RHS figure: the decay of the MSC for the different frequencies reported on the LHS bottom figure as a function of the* $10 \times 9/2 = 45$ *values of* $f^2 d^2$*. In the model given by* (8)*, the intercept is related to the SNR.*

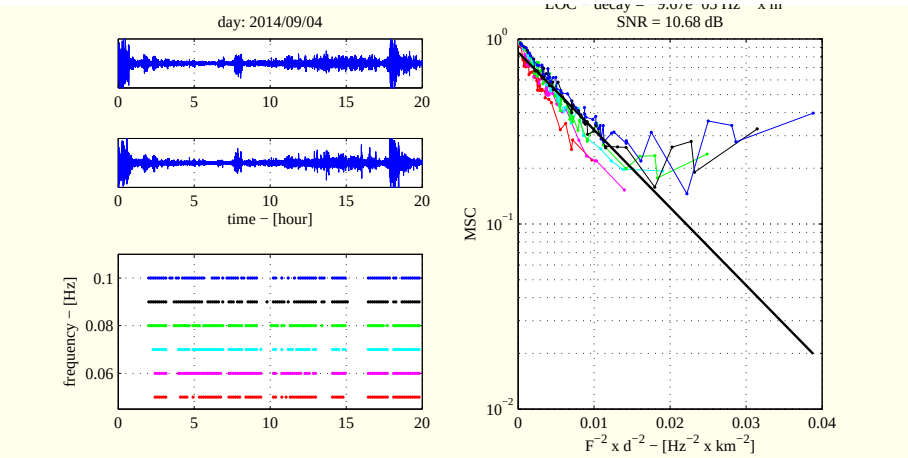

Figure 7: *LHS figures: on top, the two nearest sensor signals. Bottom: time slots where the MSC is greater than* 0.9 *for different frequencies in the band* 0.05 *Hz to* 0.1 *Hz. RHS figure: the decay of the MSC for the different frequencies reported on the LHS bottom figure as a function of the* $10 \times 9/2 = 45$ *values of* f^2d^2*. In the model given by* (8)*, the intercept is related to the SNR.*

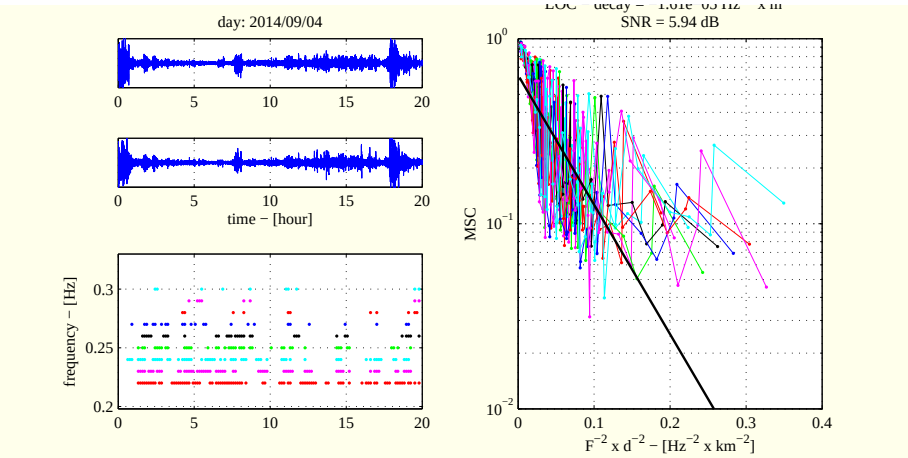

Figure 8: *LHS figures: on top, the two nearest sensor signals. Bottom: time slots where the MSC is greater than* 0.9 *for different frequencies in the band* 0.25 *Hz to* 0.3 *Hz. RHS figure: the decay of the MSC for the different frequencies reported on the LHS bottom figure as a function of the* $10 \times 9/2 = 45$ *values of* f^2d^2*. In the model given by* (8)*, the intercept is related to the SNR.*

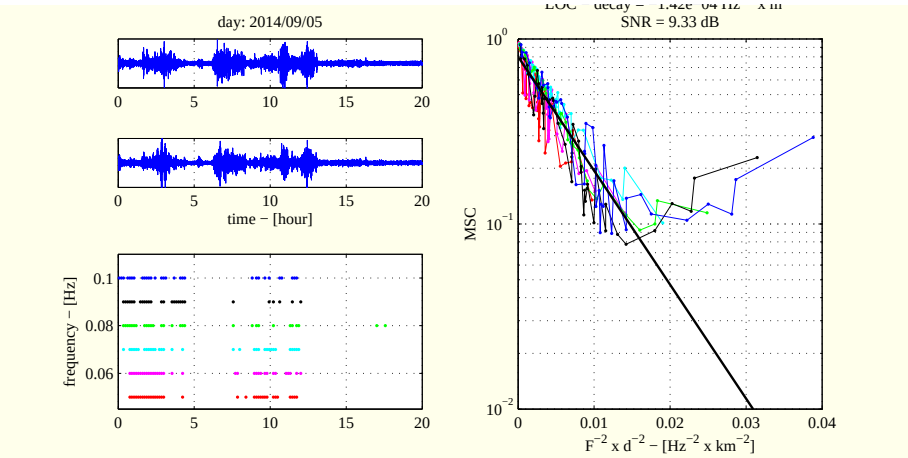

Figure 9: *LHS figures: on top, the two nearest sensor signals. Bottom: time slots where the MSC is greater than* 0.9 *for different frequencies in the band* 0.05 *Hz to* 0.1 *Hz. RHS figure: the decay of the MSC for the different frequencies reported on the LHS bottom figure as a function of the* $10 \times 9/2 = 45$ *values of* $f^2 d^2$*. In the model given by* (8)*, the intercept is related to the SNR.*

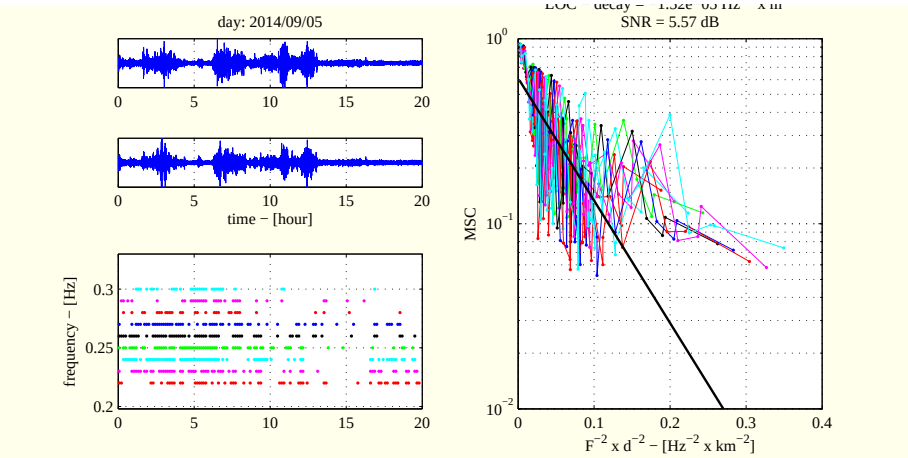

Figure 10: *LHS figures: on top, the two nearest sensor signals. Bottom: time slots where the MSC is greater than* 0.9 *for different frequencies in the band* 0.25 *Hz to* 0.3 *Hz. RHS figure: the decay of the MSC for the different frequencies reported on the LHS bottom figure as a function of the* $10 \times 9/2 = 45$ *values of* $f^2 d^2$*. In the model given by* (8)*, the intercept is related to the SNR.*

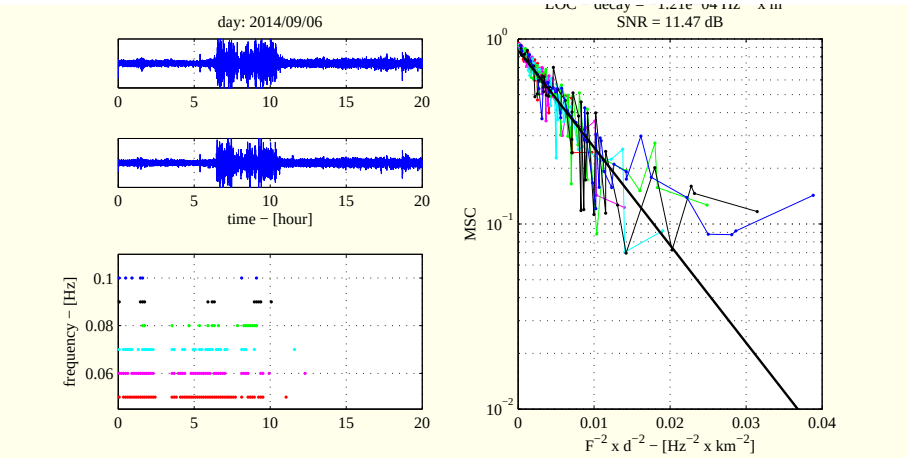

Figure 11: *LHS figures: on top, the two nearest sensor signals. Bottom: time slots where the MSC is greater than* 0.9 *for different frequencies in the band* 0.05 *Hz to* 0.1 *Hz. RHS figure: the decay of the MSC for the different frequencies reported on the LHS bottom figure as a function of the* $10 \times 9/2 = 45$ *values of* f^2d^2*. In the model given by* (8)*, the intercept is related to the SNR.*

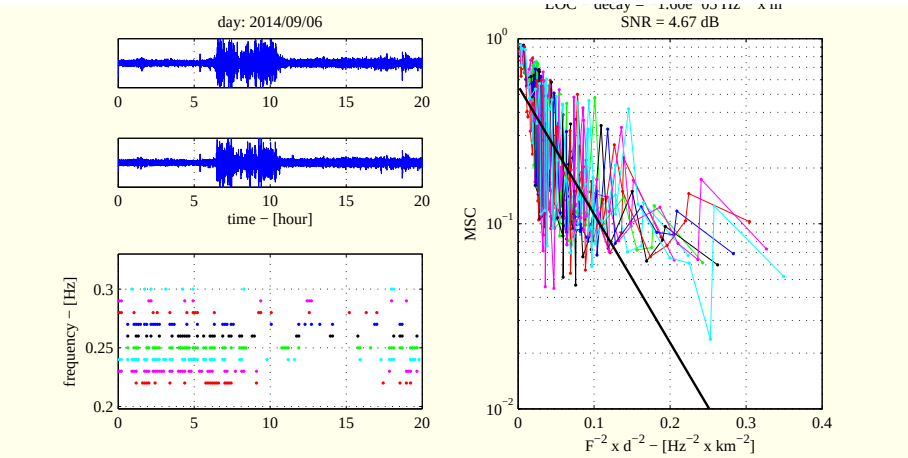

Figure 12: *LHS figures: on top, the two nearest sensor signals. Bottom: time slots where the MSC is greater than* 0.9 *for different frequencies in the band* 0.25 *Hz to* 0.3 *Hz. RHS figure: the decay of the MSC for the different frequencies reported on the LHS bottom figure as a function of the* $10 \times 9/2 = 45$ *values of* f^2d^2*. In the model given by* (8)*, the intercept is related to the SNR.*

3 Cramer-Rao bound (CRB)

Let us consider a statistical model associated to an N dimensional observation X, whose probability measure has a probability density we denote $p(x;\alpha)$ where α is a L-dimensional parameter. Then any unbiased estimator $\hat{\alpha}_N$ of α has a covariance matrix which verifies:

$$\mathbb{E}\left[(\hat{\alpha}_N - \alpha)(\hat{\alpha}_N - \alpha)^T\right] \;\leq\; \mathrm{CRB}(\alpha) = F^{-1}(\alpha)$$

where F is called the Fisher information matrix (FIM) whose (m, m') entry writes:

$$F_{m,m'} \;=\; \mathbb{E}\left[\nabla_\alpha p(x;\alpha) \nabla_\alpha^T p(x;\alpha)\right]$$

where $\nabla_\alpha p(x;\alpha)$ is the gradient of $p(x;\alpha)$ w.r.t. α. It is worth to notice that F is L dimensional square matrix.

In the Gaussian case given by the expression (9), it is shown:

$$\mathrm{FIM}_{m,m'}(\alpha) \;=\; \sum_{k=1}^{K} \mathrm{trace}\left(\Gamma_k^{-1} \times \partial_m \Gamma_k \times \Gamma_k^{-1} \times \partial_{m'} \Gamma_k\right) \tag{11}$$

where $1 \leq m, m' \leq K+4$ and where $\partial_\ell \Gamma_k$ is the partial derivative w.r.t. α. We let:

$$\dot{d}_{k,m}(\theta) \;=\; \begin{bmatrix} -2j\pi f_k r_{1,m}\, e^{-2j\pi f_k r_1^T \theta} \\ \vdots \\ -2j\pi f_k r_{M,m}\, e^{-2j\pi f_k r_M^T \theta} \end{bmatrix}$$

Then for $m = 1, 2, 3$:

$$\begin{aligned} \partial_m \Gamma_k &= \gamma_k \mathrm{diag}\left(\dot{d}_{k,m}(\theta)\right) C_k(\beta) D_k^H(\theta) + \gamma_k D_k(\theta) C_k(\beta) \mathrm{diag}\left(\dot{d}_{k,\ell}(\theta)\right)^H \\ &= 2\,\gamma_k \mathcal{R}\left(\mathrm{diag}\left(d_{k,m}(\theta)\right) C_k(\beta) D_k^H(\theta)\right) \end{aligned}$$

It is worth to notice that, if $\beta \approx +\infty$, $C_k = I_M$ and $\partial_\ell \Gamma_k = 0$ which is normal because in this case Γ_k does not depend on θ. For the derivation w.r.t. σ^2 we have:

$$\partial_4 \Gamma_k \;=\; I_M$$

A direct consequence is that the FIM, w.r.t. the components (**??**) of α is of this shape:

$$\mathrm{FIM} \;=\; \begin{bmatrix} F_{11} & F_{12} & F_{13} & 0 & 0 & \dots & 0 \\ F_{21} & F_{22} & F_{23} & 0 & 0 & \dots & 0 \\ F_{31} & F_{32} & F_{33} & 0 & 0 & \dots & 0 \\ 0 & \dots & 0 & F_{\sigma^2} & & & \\ 0 & \dots & 0 & & & & \\ \vdots & \ddots & \vdots & & & F_{\gamma,K,K} & \\ 0 & \dots & 0 & & & & \end{bmatrix}$$

Because the CRB on the estimation of θ is given by the 3×3 top-left matrix of the inverse of FIM, we are only concern with F_{123} by taking F_{123}^{-1} . Then the CRB w.r.t. the azimuth, elevation and velocity can be derived using the Jacobian of the one-to-one mapping between the slowness and the vector (a, e, c) where a, e and c denote respectively the azimut, the elevation and the velocity. The same calculation can be used to derive the CRB w.r.t. the azimuth and the trace velocity.

Appendix A

Transform an array in isotrope array

We consider an arbitrary array whose locations are given by:

$$X = \begin{bmatrix} x_{1,1} & \dots & x_{1,M} \\ x_{2,1} & \dots & x_{2,M} \\ x_{3,1} & \dots & x_{3,M} \end{bmatrix}$$

It follows that

$$XX^T = \sum_{i=1}^{d} \mu_i \xi_i \xi_i^T$$

where $0 \leq \mu_i \leq \alpha_0$. The new array writes

$$Y = \begin{bmatrix} X & \sqrt{(\alpha_0 - \mu_1)}\xi_1 & \sqrt{(\alpha_0 - \mu_2)}\xi_2 & \sqrt{(\alpha_0 - \mu_3)}\xi_3 \end{bmatrix}$$

It is easy to verify that $YY^T = \alpha_0 I_d$.

Appendix B

Coherence

The LOC is modeled by the random slowness:

$$\Theta \;=\; \theta_0 + \epsilon$$

where θ_0 is a 3D deterministic vector and ϵ a 3D random vector with zero-mean and distribution probability density denoted p_ϵ. The spectral matrix of the M-ary random vectors associated to the sensor locations has the following entry:

$$\begin{aligned} S_{\ell,\ell'}(f) &= \gamma(f) \int_{\mathbb{R}^3} e^{-2j\pi f (r_\ell - r_{\ell'})^T t} p_e(t-\theta_0) dt \\ &= \gamma(f) e^{-2j\pi f (r_\ell - r_{\ell'})^T \theta_0} \int_{\mathbb{R}^3} e^{-2j\pi f (r_\ell - r_{\ell'})^T t} p_e(t) dt \\ &= \gamma(f) e^{-2j\pi f (r_\ell - r_{\ell'})^T \theta_0} \times \Phi_e(2\pi f (r_\ell - r_{\ell'})) \end{aligned}$$

where $\Phi_e(v)$ denotes the characteristic function of the r.v. e. The deterministic case where $\epsilon = 0$ leads to:

$$S_{\ell,\ell'}(f) \;=\; \gamma(f) e^{-2j\pi f (r_\ell - r_{\ell'})^T \theta_0}$$

and therefore $S(f) = d(f) d^H(f)$ where d is a complex vector whose the ℓ-entry writes $e^{-2j\pi f r_\ell^T \theta_0}$. Hence S is a projector of rank 1 and corresponds to a pure coherent case.

In the general case:

$$S(f) \;=\; \gamma_s(f) D(f) C(f) D^H(f)$$

$D(f)$ is a diagonal matrix whose the ℓ-th diagonal entry is $e^{-2j\pi f r_\ell^T \theta_0}$ and $C(f)$ a matrix whose the (ℓ, ℓ')-entry writes:

$$C_{\ell,\ell'}(f) \;=\; \Phi_e(2\pi f (r_\ell - r_{\ell'}))$$

If ϵ is gaussian with covariance matrix Σ_θ:

$$\Phi_e(2\pi f (r_\ell - r_{\ell'})) \;=\; e^{-2\pi^2 f^2 (r_\ell - r_{\ell'})^T \Sigma_\theta (r_\ell - r_{\ell'})}$$

Σ_θ depends on 6 free parameters.

Remark 7 (Unities) *the covariance matrix Σ_θ is in s^2/m^2. It follows that $f^2\Sigma_\theta$ is homogeneous at the inverse of the wavelength square.*

Using (C.1), we can derive an expression in term of azimuth a, elevation e and velocity c. We have:

$$\Sigma_\theta = J\,\Sigma_{\text{aec}}\,J^T \tag{B.1}$$

Then

$$\begin{aligned}\log\Phi_e(2\pi f(r_\ell - r_{\ell'})) &= -2\pi^2\frac{f^2}{c^2}(r_\ell - r_{\ell'})^T K(a,e,c)\Sigma_{\text{aec}}K^T(a,e,c)(r_\ell - r_{\ell'}) \\ &= -2\pi^2(\rho_\ell - \rho_{\ell'})^T K_{\text{aec}}\Sigma_{\text{aec}}K_{\text{aec}}^T(\rho_\ell - \rho_{\ell'})\end{aligned}$$

where $\rho = r/\lambda$ with $\lambda = c/f$ and

$$K_{\text{aec}} = \begin{bmatrix}\cos(a)\cos(e) & \sin(a)\sin(e) & c^{-1}\sin(a)\cos(e) \\ -\sin(a)\cos(e) & -\cos(a)\sin(e) & -c^{-1}\cos(a)\cos(e) \\ 0 & \cos(e) & -c^{-1}\sin(e)\end{bmatrix}$$

A simple case is if we take Σ_{aec} diagonal and hence depending on only 3 free parameters.

Appendix C

One-to-one mappings and Jacobians

θ **to** (a, e, c)

If we consider the one-to-one mapping θ to (a, e, c) in $(0, 2\pi) \times (-\pi/2, \pi/2) \times \mathbb{R}^+$, we can write:

$$\begin{cases} \theta_1 = -c^{-1}\sin(a)\cos(e) & \theta_1 \in \mathbb{R} \\ \theta_2 = c^{-1}\cos(a)\cos(e) & \theta_2 \in \mathbb{R} \\ \theta_3 = c^{-1}\sin(e) & \theta_3 \in \mathbb{R} \end{cases} \quad \begin{cases} a = \arg(\theta_2 - j\theta_1) & a \in (0, 2\pi) \\ e = \arg\sin(c\theta_3) & e \in (-\pi/2, \pi/2) \\ c = (\theta_1^2 + \theta_2^2 + \theta_3^2)^{-1/2} & c \geq 0 \end{cases}$$

whose the Jacobian is

$$\begin{aligned} J(a, e, c) &= \begin{bmatrix} -c^{-1}\cos(a)\cos(e) & c^{-1}\sin(a)\sin(e) & c^{-2}\sin(a)\cos(e) \\ -c^{-1}\sin(a)\cos(e) & -c^{-1}\cos(a)\sin(e) & -c^{-2}\cos(a)\cos(e) \\ 0 & c^{-1}\cos(e) & -c^{-2}\sin(e) \end{bmatrix} \\ &= c^{-1}\begin{bmatrix} \cos(a)\cos(e) & \sin(a)\sin(e) & c^{-1}\sin(a)\cos(e) \\ -\sin(a)\cos(e) & -\cos(a)\sin(e) & -c^{-1}\cos(a)\cos(e) \\ 0 & \cos(e) & -c^{-1}\sin(e) \end{bmatrix} \\ &= c^{-1}K_{\text{aec}} \end{aligned} \tag{C.1}$$

θ **to** (a, e, v)

If we consider the one-to-one mapping θ to (a, e, v) in $(0, 2\pi) \times (-\pi/2, \pi/2) \times \mathbb{R}^+$, we can write:

$$\begin{cases} \theta_1 = -v^{-1}\sin(a) & \theta_1 \in \mathbb{R} \\ \theta_2 = v^{-1}\cos(a) & \theta_2 \in \mathbb{R} \\ \theta_3 = v^{-1}\tan(e) & \theta_3 \in \mathbb{R} \end{cases} \quad \begin{cases} a = \arg(\theta_2 - j\theta_1) & a \in (0, 2\pi) \\ e = \arg\tan(v\theta_3) & e \in (-\pi/2, \pi/2) \\ v = (\theta_1^2 + \theta_2^2)^{-1/2} & c \geq 0 \end{cases}$$

whose the Jacobian is

$$J(a, e, v) = \begin{bmatrix} -v^{-1}\cos(a) & 0 & v^{-2}\sin(a) \\ -v^{-1}\sin(a) & 0 & -v^{-2}\cos(a) \\ 0 & v^{-1}/\cos^2(e) & -v^{-2}\tan(e) \end{bmatrix} \tag{C.2}$$

Appendix D

Estimation of parameters

we have

$$\begin{aligned}\log C_{k,m,m'} &= -2\pi^2 f_k^2 (r_m - r_{m'})^T \Gamma (r_m - r_{m'}) \\ &= -2\pi^2 f_k^2 (r_{m,1} - r_{m',1})^2 \Gamma_{11} - 2\pi^2 f_k^2 (r_{m,2} - r_{m',2})^2 \Gamma_{22} - 4\pi^2 f_k^2 (r_{m,1} - r_{m',1})(r_{m,2} - r_{m',2}) \Gamma_{12} \\ &= \mu_1(k,m,m')\Gamma_{11} + \mu_2(k,m,m')\Gamma_{22} + 2\mu_3(k,m,m')\Gamma_{12}\end{aligned}$$

Enumerating $k = 1:K$, $m = 1:M$, $m' = 1:M$ with $m' > m$ leads to $KM(M-1)/2$ equations with 3 unknowns.

Appendix E

inverse of Γ_k

Here we give the analytical expression of the inverse of $\Gamma_k(\alpha) = \gamma_k D_k(\theta)\, C_k\, D_k^H(\theta) + \sigma^2 I_M$

$$\begin{aligned}\Gamma_k^{-1}(\alpha) &= \sigma^{-2} I_M - \sigma^{-4} D_k(\theta)(C_k^{-1} + \sigma^{-2} D_k^H(\theta) D_k(\theta))^{-1} D_k^H(\theta) \\ &= \sigma^{-2} I_M - \sigma^{-4} D_k(\theta)(C_k^{-1} + \sigma^{-2} I)^{-1} D_k^H(\theta)\end{aligned}$$